



**HAL**  
open science

## Structure-based design of small peptide inhibitors of protein-kinase CK2 subunit interaction

Béatrice Laudet, Caroline Barette, Vincent Dulery, Olivier Renaudet, Pascal Dumy, Alexandra Metz, Renaud Prudent, Alexandre Deshiere, Otto Dideberg, Odile Filhol, et al.

### ► To cite this version:

Béatrice Laudet, Caroline Barette, Vincent Dulery, Olivier Renaudet, Pascal Dumy, et al.. Structure-based design of small peptide inhibitors of protein-kinase CK2 subunit interaction. *Biochemical Journal*, 2007, 408 (3), pp.363-373. <10.1042/BJ20070825>. <hal-00478835>

**HAL Id: hal-00478835**

**<https://hal.science/hal-00478835v1>**

Submitted on 30 Apr 2010

**HAL** is a multi-disciplinary open access archive for the deposit and dissemination of scientific research documents, whether they are published or not. The documents may come from teaching and research institutions in France or abroad, or from public or private research centers.

L'archive ouverte pluridisciplinaire **HAL**, est destinée au dépôt et à la diffusion de documents scientifiques de niveau recherche, publiés ou non, émanant des établissements d'enseignement et de recherche français ou étrangers, des laboratoires publics ou privés.



HAL Authorization

## Structure-based design of small peptide inhibitors of protein-kinase CK2 subunit interaction

**Running Title: Inhibitors of CK2 subunit interaction.**

Béatrice LAUDET\*†‡, Caroline BARETTE§, Vincent DULERY||‡, Olivier RENAUDET||‡, Pascal DUMY||‡, Alexandra METZ\*†‡, Renaud PRUDENT\*†‡, Alexandre DESHIERE\*†‡, Otto DIDEBERG¶, Odile FILHOL\*†‡, Claude COCHET\*†‡<sup>1</sup>.

\*INSERM, U873, Grenoble, F-38054, France; †CEA, iRTSV/LTS, Grenoble, F-38054, France; ‡Université Joseph Fourier, Grenoble, France; §CEA, iRTSV/CMBA, Grenoble, F-38054, France; ||CNRS, UMR-5250, ICMG FR-2607, Grenoble, France; ¶CNRS, CEA, IBS/LCM, Grenoble, France.

<sup>1</sup>To whom correspondence should be addressed:

U873-LTS, iRTSV, CEA, 17 rue des Martyrs, 38054 Grenoble cedex 9, France.

Tel 33-4-38-78-42-04; Fax: 33-4-38-78-50-58; E-mail: [claude.cochet@cea.fr](mailto:claude.cochet@cea.fr).

---

X-ray crystallography studies as well as live-cell fluorescent imaging have recently challenged the traditional view of Protein-kinase CK2. Unbalanced expression of catalytic and regulatory CK2 subunits has been observed in a variety of tissues and tumors. Thus, the potential intersubunit flexibility suggested by these studies raises the likely prospect that the CK2 holoenzyme complex is subject to disassembly and re-assembly. In this study, we show evidence for the reversible multimeric organization of the CK2 holoenzyme complex *in vitro*. We used a combination of site-directed mutagenesis, binding experiments and functional assays to show that both *in vitro* and *in vivo*, only a small set of primary hydrophobic residues of CK2 $\beta$  which contacts at the center of the CK2 $\alpha$ /CK2 $\beta$  interface dominates affinity. The results indicate that a double mutation in CK2 $\beta$  of amino acids - Y188 and F190 – which are complementary and fill up a hydrophobic pocket of CK2 $\alpha$  is the most disruptive to CK2 $\alpha$  binding both *in vitro* and in living cells. Further characterization of hot spots in a cluster of hydrophobic amino acids centered around Y188-F190 led us to the structure-based design of small peptide inhibitors. One conformationally constrained 11-mer peptide (Pc) represents a unique CK2 $\beta$ -based small molecule that was particularly efficient

1) to antagonize the interaction between the CK2 subunits, 2) to inhibit the assembly of the CK2 holoenzyme complex, 3) to strongly affect its substrate preference.

**Key words:** CK2 protein-kinase, protein-protein interaction, cyclic peptide, peptide disruptor, hot spot, substrate specificity.

---

Abbreviations used: MBP, maltose binding protein; GST, glutathione-S-transferase; BiFC, bimolecular fluorescence complementation; YFP, yellow fluorescent protein; GFP, green fluorescent protein; FRET, fluorescence resonance energy transfer.

## INTRODUCTION

All but a handful of the protein kinase family members are monomeric enzymes which are often regulated by reversible phosphorylation. In contrast, the regulation and the molecular architecture of multi-subunit Ser/Thr protein kinases such as phosphorylase kinase [1], cAMP-dependent protein kinase [2], cyclin-dependent protein kinases [3], DNA-dependent protein kinase [4], 5'-AMP-activated protein kinase [5] and I $\kappa$ B kinase [6] rely on the reversible binding of regulatory subunits to the catalytic subunits of these enzymes. The presence of the regulatory subunit can either play a negative role on the catalytic subunit (ex. cAMP-dependent protein kinase [7]) or is a prerequisite for activation (ex. cyclin-dependent protein kinases [3]).

Protein kinase CK2 shares with few other protein kinases a quaternary structure consisting of two catalytic subunits (CK2 $\alpha$ /CK2 $\alpha'$ ) and two regulatory subunits (CK2 $\beta$ ) [8]. However, as compared to other multi-subunit protein kinases, CK2 exhibits notable distinguishing structural and functional features [9, 10]. CK2 catalytic subunits possess constitutive activity [11, 12], but CK2 $\beta$  is a central component of the tetrameric CK2 complex [13], controlling CK2 substrate specificity, cellular localization and enzymatic activity. In this respect, CK2 $\beta$  operates as a targeting subunit and/or a docking platform affecting the accessibility to the catalytic site of binding substrates whose phosphorylation is either stimulated or prevented by the CK2 $\beta$  subunit [14, 15]. In this context, the spontaneous high affinity association of recombinant CK2 subunits in a stable heterotetrameric complex (dissociation constant  $K_D = 5.4$  nM) as well as numerous complementary biochemical observations led to the long-held tenet that CK2 is a strong obligate complex. However, this traditional view was challenged when X-ray crystallography studies revealed that the CK2 $\alpha$ /CK2 $\beta$  interface is smaller than the surface contacts that are usually observed in stable protein complexes [13]. The possible intersubunit flexibility suggested by these studies was further reinforced by the observation of independent movement of CK2 $\alpha$  and CK2 $\beta$  in living cells [16]. In

addition, the presence in mouse brain and testicles of a CK2 $\beta$  fraction devoid of CK2 $\alpha$  [17] and a pool of free CK2 $\alpha$ ' in prostate tumor cells [18] have been reported. Collectively, these observations raise the likely prospect that the CK2 holoenzyme complex is subject to disassembly and re-assembly [19]. As CK2 substrates localize to many different subcellular compartments, a dynamic interaction of CK2 subunits should increase the kinase specificity and the assembly of the complex is a likely point of regulation [20]. The ability to interfere with specific protein-protein interactions has already provided powerful means of influencing the functions of selected proteins within the cell [21, 22]. Thus, the potential intersubunit flexibility of the CK2 holoenzyme complex makes it amenable to drug-discovery efforts aimed at inhibiting this protein-protein interaction.

In this work, we show evidence for the reversible multimeric organization of the CK2 holoenzyme complex *in vitro*. Site-directed mutagenesis, binding experiments and functional assays provided further insights into the molecular interaction between the CK2 subunits demonstrating that both *in vitro* and *in vivo*, only a small set of primary hydrophobic residues of CK2 $\beta$  which contacts at the center of the interface dominates affinity. Characterization of hot spots led us to a structure-based design of small peptide inhibitors derived from the CK2 $\beta$  carboxyterminal domain. One conformationally constrained 11-mer peptide can efficiently antagonize the interaction between the CK2 subunits representing the first small molecule that binds to this hydrophobic interface. This study represents the first step of a systematic approach to set the framework for the discovery and development of chemical inhibitors of this interaction.

## EXPERIMENTAL

### Materials

[ $\gamma$ - $^{32}$ P]-ATP (3,000 Ci/mmol) was purchased from MP Biosciences. The peptide substrate (RRREDEESDDEE) for CK2 kinase assay was obtained from NeomPS. The purity of this peptide (89 %) was determined by HPLC on a nucleosil C18 column using a linear triethanolamine phosphate-acetonitrile gradient. Solvents were of analytical grade. Cyclic peptides, biotinylated cyclic peptides and Ala-mutated cyclic peptides were synthesized by Eurogentec. The pEYFPc1 vector was purchased from Clontech Laboratories. EcoRI and BamHI restriction enzymes were from Invitrogen, and SacI and AgeI from New England Biolabs.

### Chemicals, peptide synthesis and purification

All chemical reagents and solvents were purchased from Sigma Aldrich, Acros or Carlo-Erba and were used without further purification. All protected amino acids were obtained from Advanced ChemTech

Europe, Bachem Biochimie SARL and France Biochem S.A.. RP-HPLC analyses were performed on Waters equipment. The analytical (Nucleosil 120 Å 3 µm C<sub>18</sub> particles, 30 x 4.6 mm<sup>2</sup>) was operated at 1.3 mL/min and the preparative (Delta-Pak 300 Å 15 µm C<sub>18</sub> particles, 200 x 25 mm<sup>2</sup>) at 22 mL/min with UV monitoring at 214 nm and 250 nm using a linear A-B gradient (buffer A: 0.09% CF<sub>3</sub>CO<sub>2</sub>H in water; buffer B: 0.09% CF<sub>3</sub>CO<sub>2</sub>H in 90% acetonitrile). Mass spectra were obtained by electron spray ionization (ESI-MS) on a VG Platform II in the positive mode.

The protected linear peptides were assembled manually on solid-phase using the standard Fmoc/*t*-Bu strategy with PyBOP<sup>®</sup> as coupling reagent on the acido labile SASRIN<sup>®</sup> resin. They were cyclized directly without further purification as reported previously [23]. For all peptides, Glycine was chosen as the C-terminal end to secure the subsequent cyclization step from epimerization. The protected cyclic peptides were finally treated with a solution of TFA/TIS/H<sub>2</sub>O (95:2.5:2.5) for two hours. After evaporation, the cyclic peptides were purified by RP-HPLC. The purified cyclic peptides were homogenous and showed expected primary ion molecular weights by mass spectrometry.

### Proteins

Human recombinant His-tagged CK2α, GST-CK2α and GFP-CK2α were obtained as previously described [16, 24]. Expression and purification of chicken recombinant MBP-CK2β was performed as previously described [25]. GST-CK2β (182-215) referred as GST-β C-ter was obtained by cloning by PCR the 33 C-terminal amino acids of CK2β in pGEX4T1. Two recombinant proteins, MBP-CDC25B (kindly provided by Bernard Ducommun, Toulouse, France) and GST-Olig2 (1-177) (personal communication, Thierry Buchou), were used as CK2β-dependent CK2 substrates.

### *In vitro* kinase assay

CK2 kinase assays were performed in a final assay volume of 18 µL containing 3 µL of CK2α (36 ng) and a mixture containing 1 mM of the peptide substrate, 10 mM MgCl<sub>2</sub>, and 1 µCi [<sup>32</sup>P]-ATP. Final concentration of ATP was 100 µM. Assays were performed under linear kinetic conditions for 5 min at RT before termination by the addition of 60 µL of 4% TCA [26].

### *In vitro* CK2α-CK2β interaction assay

The CK2α-CK2β interaction assay involved competition between plate-bound MBP-CK2β and various soluble peptides for binding to soluble [<sup>35</sup>S]-methionine-labelled CK2α. The assay was performed in Reacti-Bind streptavidin coated high binding capacity 96-well plates (Pierce) in which each well was coated with 250 ng of biotinylated MBP-CK2β (Sulfo-NHS-LC-LC-Biotin with a spacer arm of 30.5 Å

length, Pierce) in 50 mM Tris-HCl, pH 7.2, 0.4 M NaCl buffer for 1 h at RT. After 3 washes with 50 mM Tris-HCl, pH 7.2, 0.15 M NaCl, 0.05% Tween 20, the wells were blocked with 50 mM Tris-HCl, pH 7.2, 0.15M NaCl and 3% BSA for 1 h at RT. After 3 washes, competing peptides were added to each well in 50 mM Tris-HCl, pH 7.2, 0.4 M NaCl, along with [<sup>35</sup>S]-methionine-labelled CK2 $\alpha$  (10<sup>5</sup> cpm) synthesized *in vitro* by using the TnT Quick Coupled Transcription/translation System (Promega). The plates were incubated for 1 h at RT and after 3 washes, the radioactivity or the fluorescence of each well in the plate was determined using a scintillation counter. Positive control (100% competition) was determined with a 10-fold molar excess of untagged CK2 $\alpha$ , and negative control (0% competition) was performed in the absence of competitor. IC<sub>50</sub> is defined as the concentration of peptide necessary to inhibit 50% of CK2 $\alpha$ -CK2 $\beta$  complex formation.

#### **Pull-down assays**

GST-tagged proteins were immobilized on glutathione-sepharose 4 Fast Flow beads (Amersham Biosciences), for 1 h at 4°C, in 10 mM Tris-HCl, pH 7.5. Beads were then incubated with CK2 $\alpha$  for 1 h at 4°C. After 4 washes, CK2 $\alpha$  activity was measured as described above.

MBP-CK2 $\beta$  (5  $\mu$ g) was immobilized on amylose beads (New England Biolabs) for 1 h at 4°C in 10 mM NaHPO<sub>4</sub>, pH 7.2, 0.5 M NaCl, 10 mM  $\beta$ -Mercaptoethanol, 1 mM EGTA, 0.05% Tween 20. Buffer was replaced by 10 mM Tris-HCl, pH 7.5, 0.15 M NaCl, 0.05% Tween 20. Then, increasing amounts of GST- $\beta$  C-ter were added along with 5  $\mu$ g of GST-CK2 $\alpha$  for 20 min at 4°C. After 4 washes, 1/10 of beads were used for CK2 activity assay, and the remaining beads were used for CK2 $\alpha$  detection by Western-blotting.

#### **Size exclusion chromatography**

An Ultrogel ACA34 gel filtration column (0.5 x 30 cm) was equilibrated in 50 mM Tris-HCl, pH 7.5, 0.4M NaCl and calibrated using aldolase (MW = 158 kDa), bovine serum albumin (MW = 68 kDa) and carbonic anhydrase (MW = 29 kDa) as standards. CK2 $\alpha$  (50  $\mu$ g) alone or CK2 $\alpha$  (50  $\mu$ g) incubated with GST- $\beta$  C-ter (30  $\mu$ g) for 30 min at 4°C were loaded onto the column. Eluted fractions (0.25 ml) were collected and assayed for the presence of CK2 $\alpha$  and GST- $\beta$  C-ter by Western-blotting .

#### **Site-directed mutagenesis**

Site-directed mutagenesis of CK2 $\beta$  was performed with the pMALc2-CK2 $\beta$  vector using the Quick Change Site-Directed Mutagenesis kit (Stratagene) and specific primers from Eurogentec to generate different mutant MBP-CK2 $\beta$  proteins. Primers were for M166A sens 5' G TTC CCC CAT GCG CTC TTC ATG GTG 3', Y188A sens 5' GTG CCC AGG CTG GCT GGG TTC AAG ATC CAC CCT ATG G

3', F190A sens 5' GTG CCC AGG CTG TAT GGG GCC AAG ATC CAC CCT ATG G 3'. MBP-CK2 $\beta$  mutant proteins were expressed in BL21 E. coli and purified as described previously [25] and stored at -80°C in 10 mM Na<sub>2</sub>HPO<sub>4</sub>, pH 7.0, 0.5 M NaCl, 10 mM  $\beta$ -mercaptoethanol, 1 mM EGTA, and proteases inhibitors (Sigma).

### Surface Plasmon Resonance spectroscopy

Surface plasmon resonance measurements were performed using a BIAcore 3000 instrument (BIAcore AB). The running buffer was HBS (10 mM Hepes pH 7.3, 0.15 M NaCl, 3 mM EDTA, 0.005% polysorbate 20). The carboxymethylated dextran surface of a CM5 sensor chip (BIAcore AB) was activated by injecting a solution of N-hydroxysuccinimide and N-ethyl-N-(dimethylaminopropyl) carbodiimide hydrochloride (coupling solution BIAcore AB). Anti-GST antibody was diluted to 30  $\mu$ g/ml in 10 mM acetate buffer pH 5.0 and injected over the surface of the sensor chip for 7 min at a flow rate of 5  $\mu$ L/min. The unreacted sites of the sensor chip surface were then quenched by injection of 1 M ethanolamine pH 8.5. GST-CK2 $\alpha$  (50  $\mu$ g/ml) was immobilized on the surface at a flow rate of 5  $\mu$ L/min in HBS. Different MBP-CK2 $\beta$  mutants were diluted to 50  $\mu$ g/ml in HBS buffer and injected over the surface at a flow rate of 5  $\mu$ L/min. Regeneration of the surfaces was achieved by injection of 10 mM glycine-HCl pH 2.2.

### Plasmid constructs, cell transfections and BiFC analysis

Full-length chicken CK2 $\alpha$  sequence was cloned into the pEYFPc1 vector using EcoRI restriction sites, then oriented with BamHI digestion to generate the pEYFPc1-CK2 $\alpha$  construct. Full-length mouse CK2 $\beta$  sequence was cloned into the same pEYFPc1 vector using BamHI restriction sites, then oriented with EcoRI digestion to generate the pEYFPc1-CK2 $\beta$  construct. Subsequently, the EYFP sequence was substituted by the 1-154 or the 155-238 fragments of EYFP. These fragments were PCR amplified and inserted using SacI-AgeI to generate BiFC plasmid constructs. The resulting N- and C-terminal YFP-CK2 fusions are referred to as: YN-CK2 $\alpha$ , YN-CK2 $\beta$ , YC-CK2 $\alpha$ , YC-CK2 $\beta$  respectively. Primers (Eurogentec) were for YN-CK2 $\alpha$  or YN-CK2 $\beta$ : 5' G CTA CCG GTC GCC ACC ATG GTG AGC AAG 3' and 5' CAC AAC GTC TAT ATC ATG CGA GCT CAG GCT TCG AAT TCT GC 3' respectively. Primers were for YC-CK2 $\alpha$  or YC-CK2 $\beta$ : 5' CCG TCA GAT CCG CTC GCG CTA CCG GTC ATG GCC GAC AAG CAG AAG AAC GGC 3' and 5' CG AAG CTT GAG CTC GAG ATC TGA GTC CGG 3' respectively. All the constructs were verified by sequencing.

HeLa cells were grown in DMEM supplemented with 10% FCS. One day before transfection, cells were seeded in Lab-Tek chambers (Nunc) and transfected with the different BiFC plasmid constructs using

Lipofectamine 2000 reagent (Invitrogen) according to the manufacturer's instructions. Four hours after transfection, cells were washed with PBS and incubated with fresh medium for 24 h at 37°C and then switched to 30°C for 2 h to promote fluorophore maturation [27]. Preliminary experiments have shown that a fraction of YN-CK2 $\alpha$  or YC-CK2 $\alpha$  and YN-CK2 $\beta$  or YC-CK2 $\beta$  could interact with endogenous CK2 $\beta$  and CK2 $\alpha$ , trapping a part of YFP devoted to fluorescence complementation [28]. Therefore, to enhance the signal, immunostaining of YFP was performed by indirect immunofluorescence using the mouse anti-GFP antibody (Abcam) which recognizes only full-length YFP, but neither N-ter (1-154) nor C-ter (155-238) YFP (see Figure 1 in supplemental data). Under similar transfection conditions, polyclonal anti-GFP antibody (Abcam) did not discriminate between full-length and YFP-half molecules (data not shown). Thus, cells were fixed with 4% paraformaldehyde for 10 min, permeabilized with 0.5% Triton X-100 for 10 min, preincubated with 5% goat serum for 30 min at RT, and incubated with the mouse anti-GFP as primary antibody for 1 h at RT, washed with PBS and incubated with goat anti-mouse IgG-conjugated Cy3 (Molecular Probes) for 45 min at RT in the dark. Nuclei were stained by 2 $\mu$ g/ml Hoechst 33342 (Sigma) and coverslips were mounted with Dako (Dakocytomation), and examined using a Zeiss Axiovert 200 Microscope and a 40x1.3 Plan Neofluor objective. The results were expressed as % of cells that were above the fluorescence threshold observed in cells expressing only YN-CK2 $\alpha$  or YN-CK2 $\beta$ . Because the amount of expressed proteins is critical to the interpretation of results, the expression levels of the different chimeras were also analyzed in transfected cells by Western blotting using anti-CK2 $\alpha$  or CK2 $\beta$  antibodies as previously described [16, 29].

## RESULTS

### Reversibility of the CK2 subunit multimeric organization *in vitro*

Surface plasmon resonance measurements with purified recombinant CK2 $\alpha$  and CK2 $\beta$  subunits showed that they assemble rapidly ( $t_{1/2} = 60$  sec) into a stable heterotetrameric complex with nanomolar affinity ( $K_d = 5.4$  nM) with a  $k_a$  and  $k_d$  of  $6.6 \times 10^4$  M $^{-1}$  s $^{-1}$  and  $3.6 \times 10^{-4}$  s $^{-1}$  respectively [30]. However, X-ray crystallography has revealed that the CK2 $\alpha$ /CK2 $\beta$  interface was relatively small (832  $\text{\AA}^2$ ) and flexible raising the possibility that CK2 tetramers may be subjected to disassembly and re-assembly [13]. To test this hypothesis we performed a competition binding assay in which complexes between MBP-CK2 $\beta$  and [ $^{35}$ S]-methionine-labelled CK2 $\alpha$  were incubated with increasing molar excess of CK2 $\alpha$ . As shown in figure 1A, [ $^{35}$ S]-methionine-labelled CK2 $\alpha$  was efficiently displaced from the preformed complex by the CK2 $\alpha$  subunit. The residual radioactivity (15%) may represent [ $^{35}$ S]-methionine-labelled CK2 $\alpha$  present in misfolded CK2 complexes that are resistant to dissociation. In the presence of a 10-fold molar excess of

CK2 $\alpha$ , the  $t_{1/2}$  of CK2 complex dissociation was evaluated to be  $\approx$  38 min showing that unlike the fast association of CK2 subunits ( $t_{1/2} = 1$  min), the kinetic of disassembly was rather slow (figure 1B). These data are consistent with the association/dissociation rate constants determined previously [30].

### Molecular and functional analysis of the CK2 $\beta$ C-terminus

Analysis of the crystal data has revealed the major contribution of the  $\alpha/\beta$  tail contact for the stability of the CK2 holoenzyme [13]. In addition, CK2 $\beta$  mutants in which the zinc finger motif has been disrupted failed to dimerize and to recruit CK2 $\alpha$ , showing that this dimerization is essential for the proper docking of CK2 $\alpha$  [31, 32]. A CK2 $\alpha$ -interacting domain was delineated by residues 181-203 in the CK2 $\beta$  C-terminus [33]. Thus, we have expressed and purified from bacteria a CK2 $\beta$  fragment encompassing residues 182-215 fused to GST (GST- $\beta$  C-ter). Size exclusion chromatography analysis indicated that this fusion protein behaves as a dimeric protein through GST-GST interaction (data not shown). Reconstitution experiments showed that this mini protein was sufficient for a productive high-affinity interaction with CK2 $\alpha$  in a pull-down assay (Figure 2A). Size-exclusion chromatography analysis showed that the free CK2 $\alpha$  eluted as a monomer (42 kDa). In contrast, CK2 $\alpha$  incubated with GST- $\beta$  C-ter was eluted as free CK2 $\alpha$  as well as a CK2 $\alpha$ /GST- $\beta$  C-ter complex with an apparent MW of 150 kDa (Figure 2B). These data indicate that this interaction generates a stable hetero-complex bridging two catalytic subunits. Thus, the region delineated by residues 182-215 in GST- $\beta$  C-ter contains an autonomous CK2 $\alpha$ -interacting domain. We then examined the effect of this CK2 $\beta$  domain on the formation of the CK2 holoenzyme complex in a solid phase competition assay. As illustrated in Figure 2C, the interaction between CK2 $\alpha$  and CK2 $\beta$  was strongly impaired by the presence of increasing concentrations of the GST- $\beta$  C-ter protein. These results show that the 33 amino acids C-terminal region of CK2 $\beta$  binds tightly to CK2 $\alpha$  and behaves as an antagonist of the CK2 subunit interaction.

### Identification and validation of CK2 $\beta$ hot spots for high-affinity CK2 $\alpha$ binding

The crystal structure of the CK2 holoenzyme has suggested the predominant contribution of specific residues for the interfacial contacts of the CK2 $\beta$  tail with CK2 $\alpha$ , which were localized in a cluster of hydrophobic amino acids centered around Y188. As already pointed out by Niefind *et al* [14] this highly conserved segment of CK2 $\beta$  forms a structural element containing a  $\beta$ -hairpin loop with Y188 at its top (Figure 3A). This analysis provided a general outline of the CK2 $\alpha$  binding site but did not identify experimentally the specific residues involved in the binding. Guided by the high-resolution structure of the CK2 holoenzyme, we used alanine mutagenesis to target CK2 $\beta$  residues (M166, Y188, F190) in this CK2 $\alpha$ -docking site that make the most significant contacts with CK2 $\alpha$ . Residues within CK2 $\alpha$  that are

involved in interactions with these CK2 $\beta$  residues are mainly hydrophobic residues like I69, P104, Y39, L41, V42, I57, I59, V105. In addition, carbonyl oxygen of Y188 and K191 CK2 $\beta$  backbone are making H-bonds with N $\epsilon$  of Q36 and L41 of CK2 $\alpha$  respectively. However it is known that the holoenzyme structure is stable under high ionic strength, suggesting that these H-bonds may be barely involved in the subunit interaction [10]. Therefore, we tested M166A, Y188A, F190A mutants by quantitative binding analysis. Figure 4 A shows that the CK2 $\alpha$  binding activity of the single mutant F190A (CK2 $\beta$ -F) was significantly reduced and this activity was completely abrogated for the Y188A/ F190A double mutant (CK2 $\beta$ -YF) and for the M166A/Y188A/F190A triple mutant (CK2 $\beta$ -MYF). To validate these data, the binding properties of the CK2 $\beta$  mutants were also analyzed by surface plasmon resonance spectroscopy. As shown in Figure 4B, the binding activity of the CK2 $\beta$ -F single mutant was markedly decreased and the CK2 $\beta$ -YF double or the CK2 $\beta$ -MYF triple mutations virtually abolished interaction.

#### Functional properties of CK2 $\beta$ mutants

Since it is clear that in many cases, CK2 $\beta$  mediates the interaction between the catalytic subunits and its cellular substrates, thereby modulating their phosphorylation, we assumed that any mutation perturbing the CK2 subunit interaction would affect the phosphorylation of CK2 $\beta$ -dependent substrates. A functional analysis of WT CK2 $\beta$  and CK2 $\beta$ -M, CK2 $\beta$ -YF and CK2 $\beta$ -MYF mutants was performed testing their effect on the CK2-mediated phosphorylation of CDC25B [34]. The data show that, while the phosphorylation of CDC25B was weakly affected in the presence of the single CK2 $\beta$ -M mutant, the double CK2 $\beta$ -YF and triple CK2 $\beta$ -MYF mutants were inefficient for CK2-mediated phosphorylation of CDC25B (Figure 5, lanes 1-5). Similarly, autophosphorylation of the CK2 $\beta$ -YF and CK2 $\beta$ -MYF mutants was strongly affected (Figure 5, lanes 6-9) indicating that these mutants are also defective for the supramolecular organization of the CK2 holoenzyme [35]. Thus, Y188 and F190 represent key CK2 $\beta$  hot spot residues for a functional interaction with CK2 $\alpha$  *in vitro*.

#### *In vivo* validation of CK2 $\beta$ hot spots

To visualize the CK2 subunit interaction in living cells, we applied a BiFC assay (Bimolecular Fluorescence Complementation) which allows the investigation of interacting molecules *in vivo* [27]. The BiFC assay is based on the formation of a fluorescent complex by fragments of the Yellow Fluorescent Protein (YFP) brought together by the association of two interaction partners fused to non-fluorescent YFP half-molecules. This approach enables visualization of the proteins interaction under conditions that closely reflect the normal physiological environment. Previous work from our laboratory have shown that visualization of CK2 subunit interaction by fluorescence resonance energy transfer (FRET) analysis

required that the fluorochromes should be positioned on the N-terminal region of CK2 $\alpha$  and CK2 $\beta$  [36]. Thus, the (1-154; YN) and (155-238; YC) fragments of YFP were fused to the NH<sub>2</sub> terminus of CK2 $\alpha$ , CK2 $\beta$  or different CK2 $\beta$  mutants. The corresponding constructs were co-transfected in HeLa cells and the BiFC assay was performed using immunostaining of YFP to enhance the signal as described in Experimental Procedures (see also Figure 1 in supplementary data). Cells transfected with full length YFP fused to CK2 $\alpha$  (Figure 6A, panel a) or to CK2 $\beta$  (not shown) exhibit a strong fluorescence after YFP immunostaining. As expected, cells separately transfected with YN-CK2 $\alpha$ , YC-CK2 $\beta$  expression vectors (Figure 6A, panels b and c) or YN-CK2 $\beta$ , YC-CK2 $\alpha$  (not shown) did not exhibit any detectable fluorescence even after immunostaining. Co-transfection of YN-CK2 $\alpha$  and YC-CK2 $\beta$  yielded reconstitution of YFP upon specific binding in 36.8% of the cells (Figure 6A panel d and Figure 6B). When the fusion partners YN-CK2 $\alpha$  and YC-CK2 $\beta$  were cross-exchanged, reconstitution was also observed (not shown). Similarly, co-expression of YN-CK2 $\alpha$  and YC fused to CK2 $\beta$ -M, CK2 $\beta$ -Y, or CK2 $\beta$ -F single mutants allowed the observation of a characteristic fluorescent signal (Figure 6A panel e and Figure 6B). In contrast, a weak complementation (14.4% of the cells above the fluorescence threshold) was observed with CK2 $\beta$ -YF double mutant and YFP reconstitution was barely detected (2.4%) for YN fused to CK2 $\beta$ -MYF triple mutant (Figure 6A, panel f), despite strong protein expression as determined on immunoblots (Figure 6C, lanes 3, 6). These results indicate that substitutions of CK2 $\beta$  residues Y188 and F190 strongly influence the efficiency of bimolecular complex formation supporting the hypothesis that their mutation inhibit interaction with CK2 $\alpha$  in the cellular context.

### Constrained cyclic peptides as antagonists of CK2 subunit interaction

The dramatic effects of the two hot spot mutants on CK2 $\beta$  binding observed both *in vitro* and in the cellular context suggest that the interaction domain could be narrowed down to a short contiguous sequence. High-resolution structure of the CK2 holoenzyme has revealed that a cluster of well-defined hydrophobic residues present on the CK2 $\beta$  chain are facing hydrophobic residues N-terminally located at the outer surface formed by the juxtaposition of the anti-parallel  $\beta$ 4/ $\beta$ 5 sheets of CK2 $\alpha$  [13, 37]. This cluster which contains the identified hot spots Y188 and F190 represents a segment of highly conserved residues (<sup>186</sup>RLYGFKIH<sup>193</sup>) exhibiting a specific structural feature: it points away from the protein core, forms a 90°  $\beta$ -hairpin loop with Y188 at its top which binds into a shallow hydrophobic groove present in the  $\beta$ 4/ $\beta$ 5 sheets of CK2 $\alpha$  [13]. The interface relies on the steric complementarity between this CK2 $\alpha$  groove and the hydrophobic face of the CK2 $\beta$  hairloop and, in particular, on a triad of CK2 $\beta$  amino acids Y188, G189, F190 which inserts deep into the CK2 $\alpha$  groove (Figure 3A). To assess whether peptides derived from this CK2 $\beta$  region could antagonize the CK2 subunit interaction, we developed a binding

assay in which MBP-CK2 $\beta$  was bound on streptavidin-coated microtiter plates and incubated with [ $^{35}$ S]-methionine-labeled CK2 $\alpha$ . Compounds that disrupt the CK2 $\alpha$ /CK2 $\beta$  complex thus register reduced radioactivity relative to the background. We then used the X-ray structure of CK2 $\beta$  in the holoenzyme complex as a template for the design of conformationally constrained peptides derived from the CK2 $\beta$  carboxyterminal domain and centered around the Y188 and F190 hot spots. An eight residue peptide ( $^{186}$ R-H $^{193}$ ) which contained the cluster of hydrophobic residues (L187, Y188, I192) and three additional glycine residues was cyclized via two cysteines to staple its conformation and to mimic the binding face of CK2 $\beta$  with CK2 $\alpha$  (figure 3B). The biological activity of this peptide referred as Pc peptide, was first examined in a CK2 $\alpha$  pull-down assay. Figure 7A shows that the same amount of CK2 $\alpha$  activity could be found associated to biotinylated CK2 $\beta$  or biotinylated Pc indicating that this cyclic peptide stably interacts with CK2 $\alpha$ . This interaction could be also visualized by surface plasmon resonance spectroscopy (data not shown). To assess whether the Pc peptide could antagonize the CK2 subunit interaction, a CK2 subunit binding assay was performed in the presence of increasing concentrations of Pc peptide. Representative results are shown in Figure 7B. The presence of the Pc peptide strongly antagonized the formation of the CK2 complex ( $IC_{50}$  = 3  $\mu$ M). Importantly, an almost complete disassembly of the preformed complex was observed in the presence of the Pc peptide ( $IC_{50}$  = 6.5  $\mu$ M). The effect of varying the length from 8 to 14 amino acids in a series of head-to-tail cyclized peptide analogues was examined. Although all length variants significantly blocked the interaction, the eleven residue Pc peptide was the most effective (Figure 7C). Noteworthy, a linear form of Pc was much less active in this binding assay ( $IC_{50}$  = 30  $\mu$ M) and a linear form of Pc with an inverted sequence was without effect, showing that both the sequence and the constrained conformation of the peptide are essential for its antagonist activity. To explore the functional impact of each amino acid side chain on the Pc peptide antagonist activity, we synthesized a series of cyclic peptides in which each amino acid in the sequence RLYGFKIH was subjected to a systematic single-site replacement strategy. These derivatives were first tested at two fixed peptide concentrations (1.5 and 15  $\mu$ M) in the CK2 subunit interaction assay. As shown in Figure 8A, the largest effects of single alanine mutants were observed for residues F7 or G6 and to a less extent for residues Y5 and I9. Alanine substitutions of neighboring positions (R3, L4, K8, H10) caused marginal reductions in binding indicating that these residues serve a more passive role. Quantitative determination of the  $IC_{50}$  values further shows that the most disruptive alanine substitutions are confined in a small patch that extends from Y5 to F7 and the largest reduction in binding was for F7 (Figure 8B). In accord with the definition of the corresponding CK2 $\beta$  hot spots, these data highlight the importance of these residues for the biological activity of peptide Pc. A functional analysis of this peptide was performed testing its effect on the phosphorylation of the Olig-2 transcription factor which is catalyzed exclusively by the tetrameric form of CK2 (personal

communication, Thierry Buchou). Figure 9 shows that the presence of increasing concentrations of Pc led to a strong decrease of the original Olig-2 phosphorylation, reflecting a Pc-induced progressive dissociation of the catalytically active CK2 holoenzyme complex.

## DISCUSSION

The irreversible nature of the CK2 holoenzyme formation has been challenged by both its crystal structure and live cell imaging studies [13, 16]. Free populations of each CK2 subunit have been identified in several organs [17] and differential subcellular localizations have also been reported for CK2 $\alpha$  and CK2 $\beta$ . In many cases, CK2 $\beta$  operates as a docking platform affecting the accessibility of the catalytic site for binding substrates [15]. From a structural point of view, the CK2 $\beta$  subunit can provide CK2 specificity by either shielding a substantial surface of the CK2 $\alpha$  subunit or at the same time, providing a new surface near the catalytic active site. Since the free catalytic subunit and the holoenzyme exhibit divergent substrate preferences, it could be predicted that such a balance is crucial in the control of the many cellular processes that are governed by this multi-faceted enzyme [19].

Here we show that the CK2 holoenzyme complex is subject to disassembly and re-assembly *in vitro*. The rather slow rate of dissociation of the holoenzyme complex *in vitro* might not reflect the situation in intact cells where interacting partners could induce conformational changes, shifting the balance in favor of the dissociation [19]. A relatively small portion of CK2 $\beta$  encompassing the 33-residue C-terminal region constitutes a minimum CK2 $\alpha$  binding domain which is necessary and sufficient for high affinity interaction with CK2 $\alpha$ . The CK2 holoenzyme crystal structure has revealed that several residues in this domain make significant contacts with CK2 $\alpha$ . Based on these data, the finding that emerges from our mutagenesis study is that only a small set of primary hydrophobic contacts at the center of the interface dominates affinity *in vitro* allowing the identification of residues Y188 and F190 as the most important interaction points of CK2 $\beta$ . Mutations of these residues had strong functional consequences since the CK2 $\beta$ -YF and CK2 $\beta$ -MYF mutants were 1) unable to sustain the formation of a stable CK2 complex, 2) defective for its supramolecular organization and 3) inefficient for CK2-mediated phosphorylation of a CK2 $\beta$ -dependent substrate like CDC25B.

BiFC analysis from YN-CK2 $\alpha$  and YC-CK2 $\beta$  reproducibly demonstrated a specific interaction whereas the individual tagged proteins did not yield fluorescence. A characteristic BiFC pattern was detected with CK2 $\beta$ -M, CK2 $\beta$ -Y, or CK2 $\beta$ -F single mutants indicating that these CK2 $\beta$  mutants mediate CK2 $\alpha$  recognition. In contrast, BiFC fluorescence could be monitored only at a very low intensity with CK2 $\beta$ -YF double mutant demonstrating that these two amino acids are essential for a productive complex

formation in the normal cellular environment. These observations which corroborated our *in vitro* quantitative binding analysis were supportive of the ability to design peptides that can affect the CK2 subunit interaction. This led us to a structure-based design of CK2 $\beta$ -derived conformationally constrained peptides that can efficiently antagonize this high affinity interaction. Among a series of cyclic peptides, the disulfide bridged Pc peptide was the most active peptide variant. This cyclic peptide was considerably more potent than its identical linear form, indicating that cyclization staples the peptide in a fixed conformation, a strategy that is known to strongly enhance peptide affinity for their target by limiting flexibility and multiple conformational changes [38]. Consistent with the identification of Y188 and F190 as CK2 $\beta$  hot spots, alanine-scanning analysis has confirmed that change of these two hydrophobic residues was highly detrimental for the inhibitory activity of the Pc peptide.

### Potential biological relevance of CK2 subunit antagonists

To our knowledge, the 11-mer peptide Pc represents the first small antagonist that binds to the CK2 interface and inhibits its high affinity subunit interaction. Functional analysis showed that Pc could act as an antagonist of CK2 $\beta$ -dependent phosphorylation through the inhibition/disruption of the CK2 holoenzyme complex. Structural modifications of this cyclic peptide such as attachment to cell permeable adducts will be required to confer *in vivo* activity. Future efforts should also focus on the design of peptidomimetics with enhanced activity and selectivity.

Alternatively, our study further indicates that it should be possible to obtain small chemical molecules that bind to the CK2 $\alpha$  hydrophobic groove and inhibit its interaction with CK2 $\beta$  in a manner similar to the Pc peptide. Molecules that selectively inhibit the CK2 subunit interaction would be useful in determining the importance of CK2 $\beta$  in the control of the many cellular processes that are governed by this multifunctional kinase. In particular, such inhibitors would provide more rapid and reversible tools than siRNA or overexpression methods for correctly identifying relevant CK2 $\beta$ -dependent substrates. They will also serve as leads for the rational design of function-specific drugs that disrupt some actions of CK2, but leave other intact, allowing to deregulate specific intracellular pathways. Furthermore, selective disruption of the CK2 $\alpha$ /CK2 $\beta$  interaction could find important applications to pharmacologically test the importance of this interaction in tumor cell growth. With the help of structure-based rational design, the idea of finding small chemical molecules with significantly higher affinities for CK2 $\alpha$  using the Pc peptide as a lead molecule does not seem far-fetched.

### FOOTNOTES

We thank Thierry Buchou for providing recombinant GST-Olig2, Jean-Baptiste Raiser for assistance in molecular modelling, Nicole Thielens for assistance in BIAcore and Bernard Ducommun for providing recombinant CDC25B. This work was supported by the Institut National de la Santé et de la Recherche Médicale (INSERM), the Commissariat à l'Énergie Atomique (CEA), the Ligue Nationale contre le Cancer (Equipe labellisée 2007), and the Institut National du Cancer (grant n°57) and by the Centre National pour la Recherche Scientifique (CNRS) and the Université Joseph Fourier (UJF). We also acknowledge the Plateau de Synthèse de la Plate-Forme Chimie Nanobio and the Ministère de la Recherche for grant No. 15432-2004 to V.D.

## REFERENCES

- 1 Andreeva, I. E., Livanova, N. B., Eronina, T. B., Silonova, G. V. and Poglazov, B. F. (1986) Phosphorylase kinase from chicken skeletal muscle. Quaternary structure, regulatory properties and partial proteolysis. *Eur. J. Biochem.* **158**, 99-106
- 2 Gibson, R. M., Ji-Buechler, Y. and Taylor, S. S. (1997) Interaction of the regulatory and catalytic subunits of cAMP-dependent protein kinase. Electrostatic sites on the type Ialpha regulatory subunit. *J. Biol. Chem.* **272**, 16343-16350
- 3 Nigg, E. A. (1995) Cyclin-dependent protein kinases: key regulators of the eukaryotic cell cycle. *Bioessays.* **17**, 471-480
- 4 Hsu, H. L., Yannone, S. M. and Chen, D. J. (2002) Defining interactions between DNA-PK and ligase IV/XRCC4. *DNA Repair (Amst).* **1**, 225-235
- 5 Dyck, J. R., Gao, G., Widmer, J., Stapleton, D., Fernandez, C. S., Kemp, B. E. and Witters, L. A. (1996) Regulation of 5'-AMP-activated protein kinase activity by the noncatalytic beta and gamma subunits. *J. Biol. Chem.* **271**, 17798-17803
- 6 Rothwarf, D. M., Zandi, E., Natoli, G. and Karin, M. (1998) IKK-gamma is an essential regulatory subunit of the I $\kappa$ B kinase complex. *Nature.* **395**, 297-300
- 7 Gibson, R. M. and Taylor, S. S. (1997) Dissecting the cooperative reassociation of the regulatory and catalytic subunits of cAMP-dependent protein kinase. Role of Trp-196 in the catalytic subunit. *J. Biol. Chem.* **272**, 31998-32005
- 8 Pinna, L. A. (2002) Protein kinase CK2: a challenge to canons. *J. Cell. Sci.* **115**, 3873-3878
- 9 Allende, J. E. and Allende, C. C. (1995) Protein kinases. 4. Protein kinase CK2: an enzyme with multiple substrates and a puzzling regulation. *Faseb J.* **9**, 313-323
- 10 Litchfield, D. W. (2003) Protein kinase CK2: structure, regulation and role in cellular decisions of life and death. *Biochem. J.* **369**, 1-15

- 11 Hu, E. and Rubin, C. S. (1990) Expression of wild-type and mutated forms of the catalytic (alpha) subunit of *Caenorhabditis elegans* casein kinase II in *Escherichia coli*. *J. Biol. Chem.* **265**, 20609-20615
- 12 Grankowski, N., Boldyreff, B. and Issinger, O. G. (1991) Isolation and characterization of recombinant human casein kinase II subunits alpha and beta from bacteria. *Eur. J. Biochem.* **198**, 25-30
- 13 Niefind, K., Guerra, B., Ermakowa, I. and Issinger, O. G. (2001) Crystal structure of human protein kinase CK2: insights into basic properties of the CK2 holoenzyme. *Embo J.* **20**, 5320-5331
- 14 Chantalat, L., Leroy, D., Filhol, O., Nueda, A., Benitez, M. J., Chambaz, E. M., Cochet, C. and Dideberg, O. (1999) Crystal structure of the human protein kinase CK2 regulatory subunit reveals its zinc finger-mediated dimerization. *Embo J.* **18**, 2930-2940
- 15 Bibby, A. C. and Litchfield, D. W. (2005) The Multiple Personalities of the Regulatory Subunit of Protein Kinase CK2: CK2 Dependent and CK2 Independent Roles Reveal a Secret Identity for CK2beta. *Int. J. Biol. Sci.* **1**, 67-79
- 16 Filhol, O., Nueda, A., Martel, V., Gerber-Scokaert, D., Benitez, M. J., Souchier, C., Saoudi, Y. and Cochet, C. (2003) Live-cell fluorescence imaging reveals the dynamics of protein kinase CK2 individual subunits. *Mol. Cell. Biol.* **23**, 975-987
- 17 Guerra, B., Siemer, S., Boldyreff, B. and Issinger, O. G. (1999) Protein kinase CK2: evidence for a protein kinase CK2beta subunit fraction, devoid of the catalytic CK2alpha subunit, in mouse brain and testicles. *FEBS Lett.* **462**, 353-357
- 18 Li, X., Guan, B., Maghami, S. and Bieberich, C. J. (2006) NKX3.1 is regulated by protein kinase CK2 in prostate tumor cells. *Mol. Cell. Biol.* **26**, 3008-3017
- 19 Filhol, O., Martiel, J. L. and Cochet, C. (2004) Protein kinase CK2: a new view of an old molecular complex. *EMBO Rep.* **5**, 351-355
- 20 Allende, C. C. and Allende, J. E. (1998) Promiscuous subunit interactions: a possible mechanism for the regulation of protein kinase CK2. *J. Cell. Biochem. Suppl.* **30-31**, 129-136
- 21 Berg, T. (2003) Modulation of protein-protein interactions with small organic molecules. *Angew. Chem. Int. Ed. Engl.* **42**, 2462-2481
- 22 Chene, P. (2006) Drugs targeting protein-protein interactions. *ChemMedChem.* **1**, 400-411
- 23 Renaudet, O. and Dumy, P. (2003) Chemoselectively template-assembled glycoconjugates as mimics for multivalent presentation of carbohydrates. *Org. Lett.* **5**, 243-246
- 24 Heriche, J. K., Lebrin, F., Rabilloud, T., Leroy, D., Chambaz, E. M. and Goldberg, Y. (1997) Regulation of protein phosphatase 2A by direct interaction with casein kinase 2alpha. *Science.* **276**, 952-955

- 25 Leroy, D., Filhol, O., Quintaine, N., Sarrouilhe, D., Loue-Mackenbach, P., Chambaz, E. M. and Cochet, C. (1999) Dissecting subdomains involved in multiple functions of the CK2beta subunit. *Mol. Cell. Biochem.* **191**, 43-50
- 26 Filhol, O., Cochet, C., Wedegaertner, P., Gill, G. N. and Chambaz, E. M. (1991) Coexpression of both alpha and beta subunits is required for assembly of regulated casein kinase II. *Biochemistry.* **30**, 11133-11140
- 27 Hu, C. D. and Kerppola, T. K. (2003) Simultaneous visualization of multiple protein interactions in living cells using multicolor fluorescence complementation analysis. *Nat. Biotechnol.* **21**, 539-545
- 28 Kerppola, T. K. (2006) Visualization of molecular interactions by fluorescence complementation. *Nat. Rev. Mol. Cell. Biol.* **7**, 449-456
- 29 Martel, V., Filhol, O., Colas, P. and Cochet, C. (2006) p53-dependent inhibition of mammalian cell survival by a genetically selected peptide aptamer that targets the regulatory subunit of protein kinase CK2. *Oncogene.* **25**, 7343-7353
- 30 Martel, V., Filhol, O., Nueda, A. and Cochet, C. (2002) Dynamic localization/association of protein kinase CK2 subunits in living cells: a role in its cellular regulation? *Ann. N. Y. Acad. Sci.* **973**, 272-277
- 31 Canton, D. A., Zhang, C. and Litchfield, D. W. (2001) Assembly of protein kinase CK2: investigation of complex formation between catalytic and regulatory subunits using a zinc-finger-deficient mutant of CK2beta. *Biochem. J.* **358**, 87-94
- 32 Filhol, O., Benitez, M.J., Cochet, C. (2004) A Zinc ribbon motif is essential for the formation of functional tetrameric protein kinase CK2. *Biosciences*, 124-129
- 33 Marin, O., Meggio, F., Sarno, S. and Pinna, L. A. (1997) Physical dissection of the structural elements responsible for regulatory properties and intersubunit interactions of protein kinase CK2 beta-subunit. *Biochemistry.* **36**, 7192-7198
- 34 Theis-Febvre, N., Filhol, O., Froment, C., Cazales, M., Cochet, C., Monsarrat, B., Ducommun, B. and Baldin, V. (2003) Protein kinase CK2 regulates CDC25B phosphatase activity. *Oncogene.* **22**, 220-232
- 35 Pagano, M. A., Sarno, S., Poletto, G., Cozza, G., Pinna, L. A. and Meggio, F. (2005) Autophosphorylation at the regulatory beta subunit reflects the supramolecular organization of protein kinase CK2. *Mol. Cell. Biochem.* **274**, 23-29
- 36 Theis-Febvre, N., Martel, V., Laudet, B., Souchier, C., Grunwald, D., Cochet, C. and Filhol, O. (2005) Highlighting protein kinase CK2 movement in living cells. *Mol. Cell. Biochem.* **274**, 15-22

- 37 Ermakova, I., Boldyreff, B., Issinger, O. G. and Niefind, K. (2003) Crystal structure of a C-terminal deletion mutant of human protein kinase CK2 catalytic subunit. *J. Mol. Biol.* **330**, 925-934
- 38 Leduc, A. M., Trent, J. O., Wittliff, J. L., Bramlett, K. S., Briggs, S. L., Chirgadze, N. Y., Wang, Y., Burris, T. P. and Spatola, A. F. (2003) Helix-stabilized cyclic peptides as selective inhibitors of steroid receptor-coactivator interactions. *Proc. Natl. Acad. Sci. U S A.* **100**, 11273-11278
- 39 Emsley, P. and Cowtan, K. (2004) Coot: model-building tools for molecular graphics. *Acta Crystallogr. D. Biol. Crystallogr.* **60**, 2126-2132
- 40 Vagin, A. A., Steiner, R. A., Lebedev, A. A., Potterton, L., McNicholas, S., Long, F. and Murshudov, G. N. (2004) REFMAC5 dictionary: organization of prior chemical knowledge and guidelines for its use. *Acta Crystallogr. D. Biol. Crystallogr.* **60**, 2184-2195
- 41 (1994) The CCP4 suite: programs for protein crystallography. *Acta. Crystallogr. D. Biol. Crystallogr.* **50**, 760-763
- 42 Pettersen, E. F., Goddard, T. D., Huang, C. C., Couch, G. S., Greenblatt, D. M., Meng, E. C. and Ferrin, T. E. (2004) UCSF Chimera--a visualization system for exploratory research and analysis. *J. Comput. Chem.* **25**, 1605-1612

## FIGURE LEGENDS

### Figure 1 Reversibility of the CK2 subunit assembly *in vitro*

(A) Exchange of CK2 $\alpha$  in the subunit complex. Preformed complexes between immobilized MBP-CK2 $\beta$  and [<sup>35</sup>S]-methionine-labelled-CK2 $\alpha$  were incubated for 1h with increasing concentrations of unlabelled CK2 $\alpha$ . After washing, the amount of [<sup>35</sup>S]-methionine-labelled-CK2 $\alpha$  present in the complex was determined by radioactivity counting. (B) Kinetic of dissociation of the CK2 subunit complex. Preformed complexes between [<sup>35</sup>S]-methionine-labelled-CK2 $\alpha$  and MBP-CK2 $\beta$  were incubated for different time with a 10-fold molar excess of unlabelled CK2 $\alpha$ . After washing, the amount of [<sup>35</sup>S]-methionine-labelled-CK2 $\alpha$  remaining in the complex was determined by radioactivity counting. Results are the means  $\pm$  S.D. (n = 3).

### Figure 2 Interaction of a CK2 $\beta$ C-terminal fragment with CK2 $\alpha$

(A) Stable association of CK2 $\alpha$  with a GST- $\beta$  C-ter fragment. Agarose beads containing different GST-tagged proteins were incubated with or without CK2 $\alpha$  as indicated. After washing, the amount of associated CK2 $\alpha$  was evaluated by CK2 kinase assay as described in the experimental section. (B) Size

exclusion chromatography of either free CK2 $\alpha$  (upper panel) or CK2 $\alpha$ /GST- $\beta$  C-ter complex (lower panel). Collected fractions were assayed for the presence of CK2 $\alpha$  by Western blotting. Elution of molecular weight standards is indicated. (C) Antagonist effect of the GST- $\beta$  C-ter fragment. Immobilized MBP-CK2 $\beta$  was incubated with the indicated fold excess of GST- $\beta$  C-ter and a fixed amount of CK2 $\alpha$ . After washing, the amount of associated CK2 $\alpha$  was assessed by CK2 kinase assay and Western blotting.

### Figure 3 Structure and mode of binding of Pc peptide on CK2 $\alpha$

(A) Surface representation of the binding pocket of CK2 $\alpha$  interacting with a short C-terminal loop of CK2 $\beta$ . Crystal structure of the CK2 holoenzyme shows that a C-terminal fragment of the CK2 $\beta$ 1 chain encompassing residues 186-193 (colored in green) forms a loop inserting into a deep hydrophobic pocket of CK2 $\alpha$  [14]. Surface representation of the CK2 $\alpha$  cleft in grey highlights its pocket-like characteristics. The phenyl and phenol rings of the two non-polar and aromatic CK2 $\beta$  residues Y188 and F190 respectively (colored in red), are in quasi planar opposite orientation and fit tightly in it. M166 (colored in red) located on the second CK2 $\beta$ 2 chain (colored in yellow) is labeled. (B) Molecular model of Pc peptide in CK2 $\alpha$  pocket. A rough molecular model of Pc peptide (in blue) was obtained from the CK2 $\beta$ 1 structure previously determined (PDB code 1JWH, [13]). In details, the CK2 $\beta$ 1 structure segment (<sup>186</sup>RLYGFKIH<sup>193</sup> in green) was taken as template for the corresponding central peptide segment and the terminal aminoacids were manually added using the program Coot [39]. A basic geometric idealization of peptide bonds was then performed using the program Refmac 5 [40] from Ccp4 [41]. For clarity, only key interacting residues of CK2 $\beta$ 1 are shown (in red). The cystein disulfide bridge is colored in orange. The superimposition of Pc peptide with the CK2 $\beta$ -C-terminal loop demonstrates that Pc emulates the interaction of the natural ligand CK2 $\beta$  with CK2 $\alpha$ . Pictures were prepared with the Chimera software [42] and the 1JWH PDB structure [14].

### Figure 4 CK2 $\alpha$ binding activity of CK2 $\beta$ mutant proteins

(A) Solid phase CK2 $\alpha$  binding assay of different CK2 $\beta$  mutants. Immobilized WT CK2 $\beta$  was incubated with [<sup>35</sup>S]-methionine-labelled CK2 $\alpha$  in the presence of increasing concentrations of soluble WT MBP-CK2 $\beta$  or MBP-CK2 $\beta$  mutants as indicated. After washing, the amount of associated CK2 $\alpha$  was evaluated by radioactivity counting. Results are the means  $\pm$  S.D. (n = 3). (B) Real time binding kinetics between immobilized GST-CK2 $\alpha$  and different MBP-CK2 $\beta$  mutant proteins measured by surface plasmon resonance. The interaction between immobilized GST-CK2 $\alpha$  and MBP-CK2 $\beta$  mutants was recorded as described in Experimental Procedures.

### Figure 5 Phosphorylation of CDC25B by CK2 $\alpha$ in presence of CK2 $\beta$ or CK2 $\beta$ mutants

MBP-CDC25B (1.5  $\mu$ M) was pre-incubated for 15 min with CK2 $\alpha$  (0.6  $\mu$ M) in the presence of 0.35  $\mu$ M of WT MBP-CK2 $\beta$  or the indicated MBP-CK2 $\beta$  mutants. Phosphorylation reaction was carried out for 5 min at RT in the presence of 25  $\mu$ M [ $\gamma$ <sup>32</sup>P]-ATP-MgCl<sub>2</sub>. Phosphorylated proteins were separated on SDS PAGE and analyzed by autoradiography (upper panel) or Coomassie staining (lower panel). 1: CDC25B, 2: WT MBP-CK2 $\beta$  + CDC25B, 3: MBP-CK2 $\beta$ -M + CDC25B, 4: MBP-CK2 $\beta$ -YF + CDC25B, 5: MBP-CK2 $\beta$ -MYF + CDC25B, 6: WT MBP-CK2 $\beta$ , 7: MBP-CK2 $\beta$ -M, 8: MBP-CK2 $\beta$ -YF, 9: MBP-CK2 $\beta$ -MYF.

### Figure 6 Visualization of interactions between CK2 $\alpha$ and CK2 $\beta$ or CK2 $\beta$ mutants in living cells by Bimolecular Fluorescence Complementation

(A) Immunofluorescence images of HeLa cells transfected with plasmids expressing the YFP fragments fused to CK2 $\alpha$ , CK2 $\beta$  or CK2 $\beta$  mutants as indicated in each panel. Twenty four hours after transfection, immunostaining of YFP was performed to enhance the signal as described in Experimental Procedures. The diagrams on the left of the images represent the experimental strategies used. (B) Quantification of the BiFC signal in cells co-transfected with different plasmid constructs. Results are expressed as % of cells that were above the fluorescence threshold observed in cells expressing only YN-CK2 $\alpha$  or YN-CK2 $\beta$ . (C) Western blot analysis of the levels of protein expression. Cells corresponding to panels d, e, f in Figure 6A that expressed the indicated proteins were harvested, and the cell extracts were analysed by Western blotting using anti-CK2 $\alpha$  (lanes 1, 2, 3) and CK2 $\beta$  (lanes 4, 5, 6) antibodies. Lanes 1, 4: YN-CK2 $\alpha$  + WT YC-CK2 $\beta$ , lanes 2, 5: YN-CK2 $\alpha$  + YC-CK2 $\beta$ -M, lanes 3, 6: YN-CK2 $\alpha$  + YC-CK2 $\beta$ -MYF.

### Figure 7 Disruption of CK2 subunits interaction by CK2 $\beta$ -derived cyclic peptides

(A) Binding of Pc peptide or CK2 $\beta$  to CK2 $\alpha$ . Increasing concentrations of biotinylated Pc peptide (-▲-) or biotinylated MBP-CK2 $\beta$  (-Δ-) were immobilized on streptavidin beads and incubated with CK2 $\alpha$  (0.3  $\mu$ M) for 15 min at 4°C. After washing, the amount of associated CK2 $\alpha$  was evaluated by CK2 kinase assay. (B) Inhibition of CK2 $\alpha$ /CK2 $\beta$  complex formation by Pc peptide (-▲-). Immobilized MBP-CK2 $\beta$  was incubated with increasing concentrations of Pc peptide, followed by the addition of [<sup>35</sup>S]-methionine-labelled CK2 $\alpha$  (10<sup>5</sup> cpm). After washing, bound CK2 $\alpha$  was determined by radioactivity counting. Dissociation of preformed CK2 $\alpha$ /CK2 $\beta$  complex by Pc peptide (-■-). [<sup>35</sup>S]-methionine-labelled CK2 $\alpha$  was incubated with immobilized MBP-CK2 $\beta$ , followed by the addition of increasing concentrations of Pc peptide. After washing, bound CK2 $\alpha$  was determined by radioactivity counting. (C) Inhibition of CK2 $\alpha$ /CK2 $\beta$  complex formation by different Pc peptide derivatives. Increasing concentrations of the

different peptides were tested as in (B). Pc (-▲-), Linear peptide GAGGRLYGFKIHGGP (-■-), inverted linear peptide PGGHIKFGYLRGGAG (-Δ-), Head-to-tail peptide analogues: PcL1 RLYGFKIHHPGAGG (-□-), PcL2 RLYGFKIHGPGAGG (-●-) and PcL3 RLYGFKIHGGPGAGG (-○-). Results are the means  $\pm$  S.D. (n = 3).

### Figure 8 Antagonist effects of peptide Pc variants carrying single-site mutations

(A) Various Pc peptide variants generated by alanine scanning were tested at 1.5  $\mu$ M (□) or 15  $\mu$ M (■) for their antagonist effect on the association of CK2 subunits as described in figure 7C. The mean and standard deviation (n = 3) of representative experiment are shown. (B) IC<sub>50</sub> values determined for each peptide variant.

### Figure 9 Antagonist effect of Pc peptide on CK2-mediated phosphorylation of a CK2 $\beta$ -dependent substrate

Preformed CK2 complexes were incubated for 15 min at 4°C with increasing concentrations of Pc peptide followed by the addition of GST-Olig2 (5  $\mu$ g) and 25  $\mu$ M [ $\gamma$ <sup>32</sup>P]-ATP-MgCl<sub>2</sub> for 5 min at RT. Phosphorylated proteins were separated on SDS-PAGE and analyzed by autoradiography (upper panel) or Coomassie staining (lower panel). The results are representative of two independent experiments. C: control without CK2.

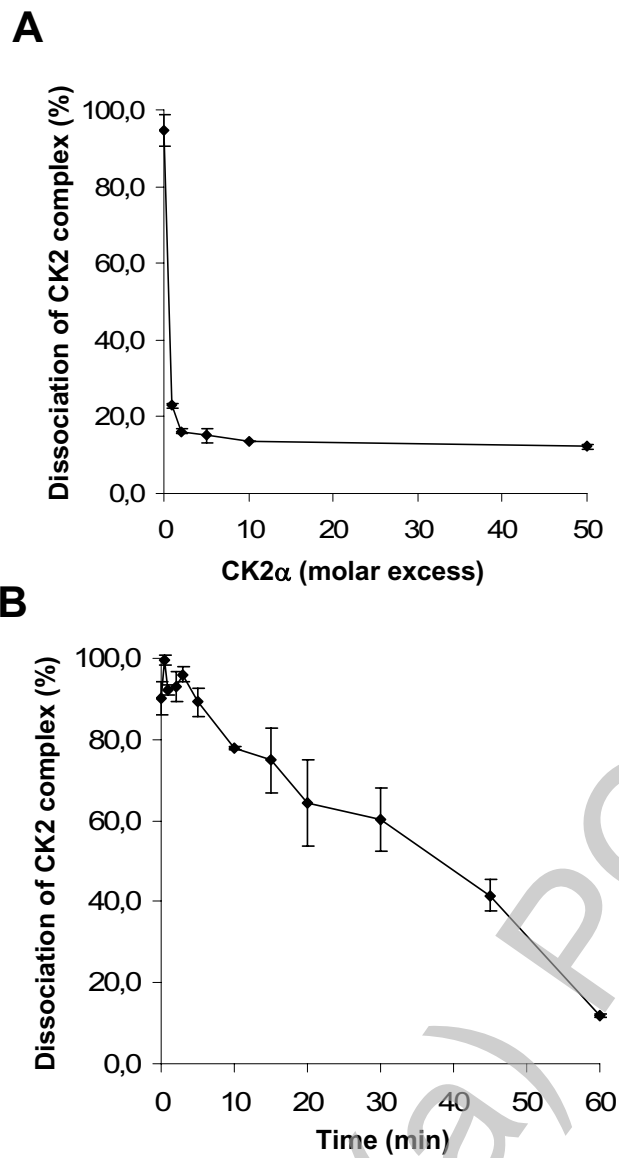
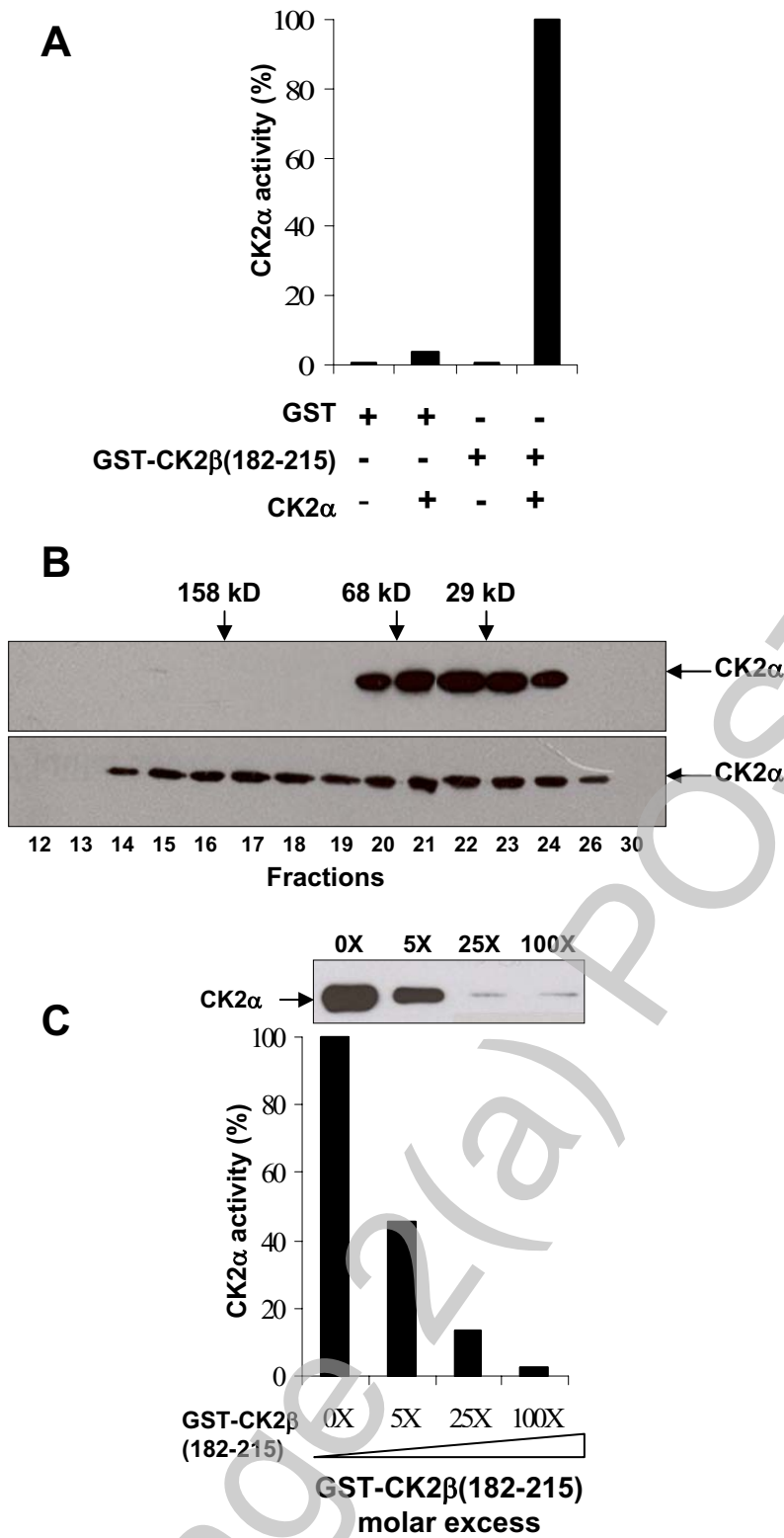


Figure 1



**Figure 2**

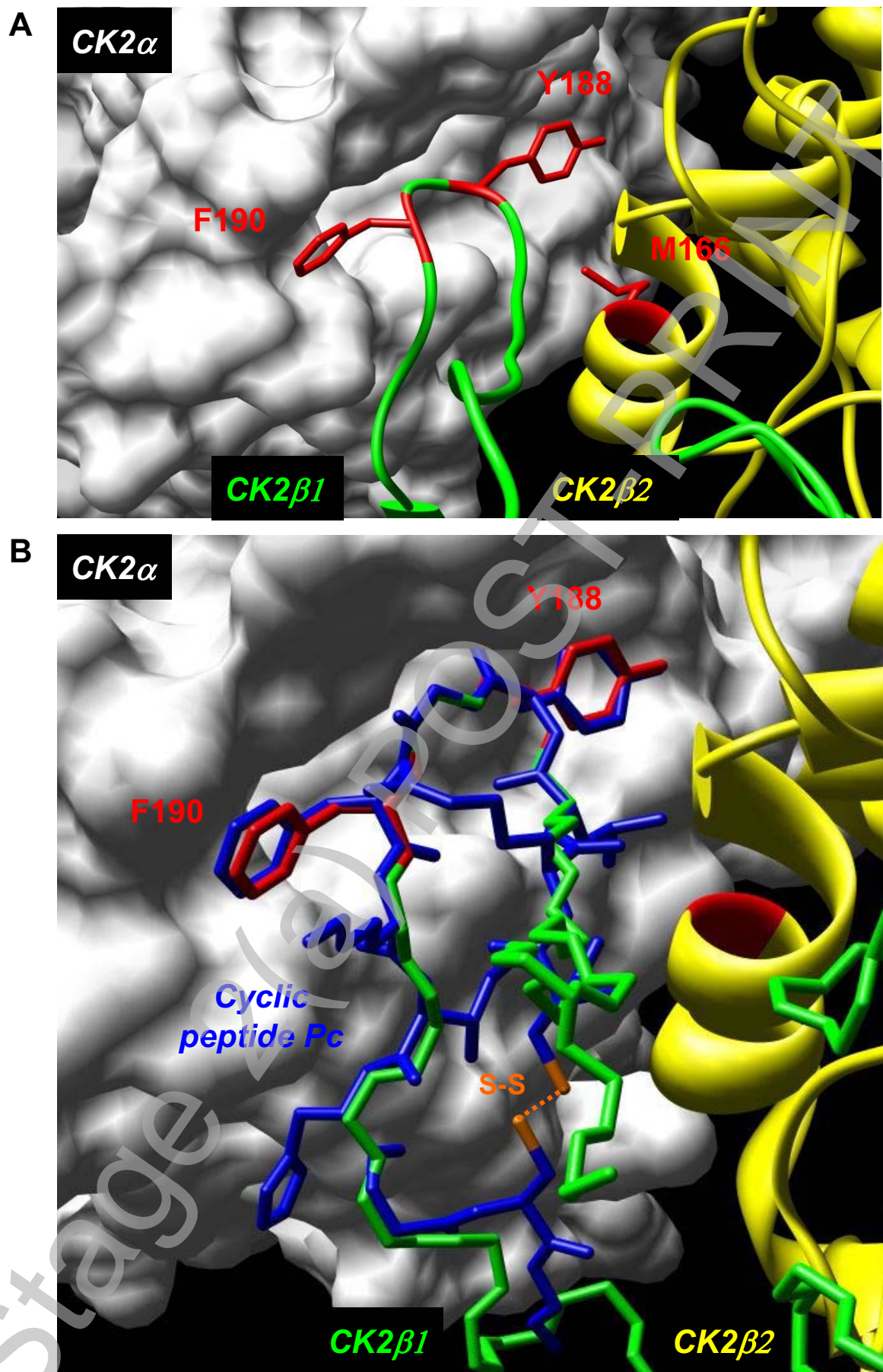
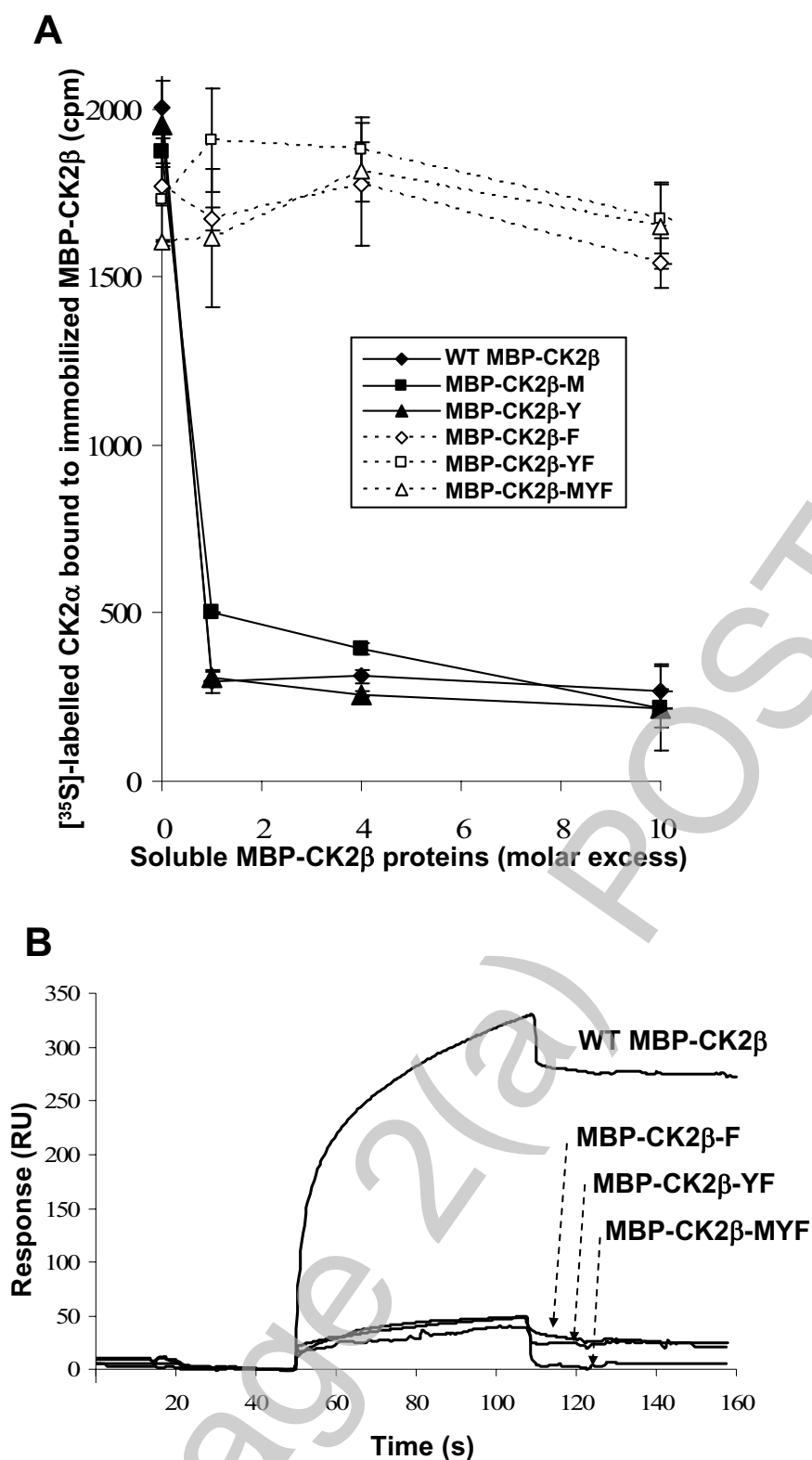
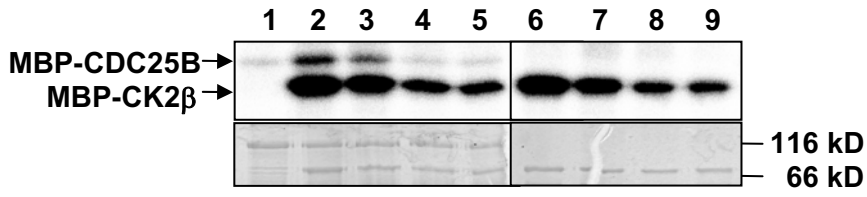


Figure 3

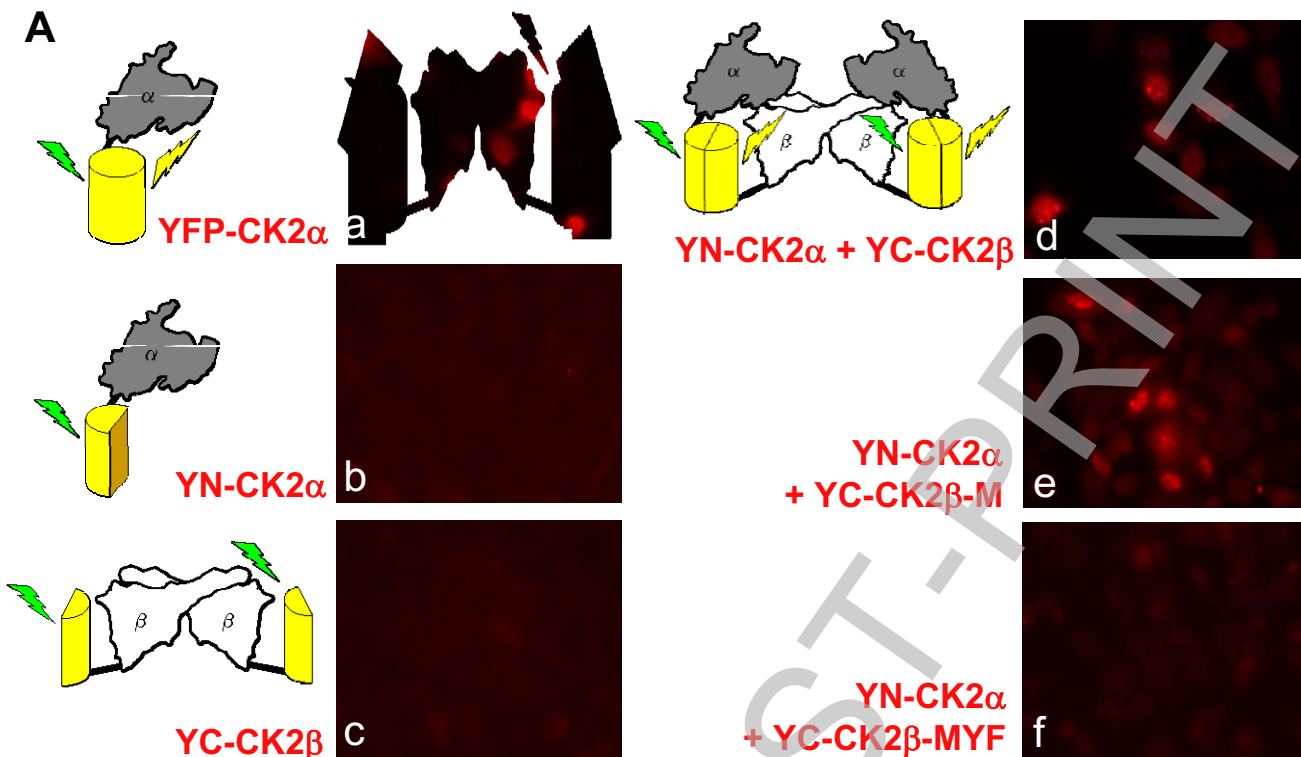




**Figure 5**

Stage 2(a) POST-PRINT

THIS IS NOT THE FINAL VERSION - see doi:10.1042/BJ20070825



**B**

Co-transfection	YFP complementation
YN-CK2 $\alpha$ + YC-CK2 $\beta$	36,8 %
YN-CK2 $\alpha$ + YC-CK2 $\beta$ M	20,5 %
YN-CK2 $\alpha$ + YC-CK2 $\beta$ YF	14,4 %
YN-CK2 $\alpha$ + YC-CK2 $\beta$ MYF	2,4 %
YC-CK2 $\alpha$ + YN-CK2 $\beta$	22,6 %
YC-CK2 $\alpha$ + YN-CK2 $\beta$ M	26,2 %
YC-CK2 $\alpha$ + YN-CK2 $\beta$ YF	9,6 %
YC-CK2 $\alpha$ + YN-CK2 $\beta$ MYF	2,4 %

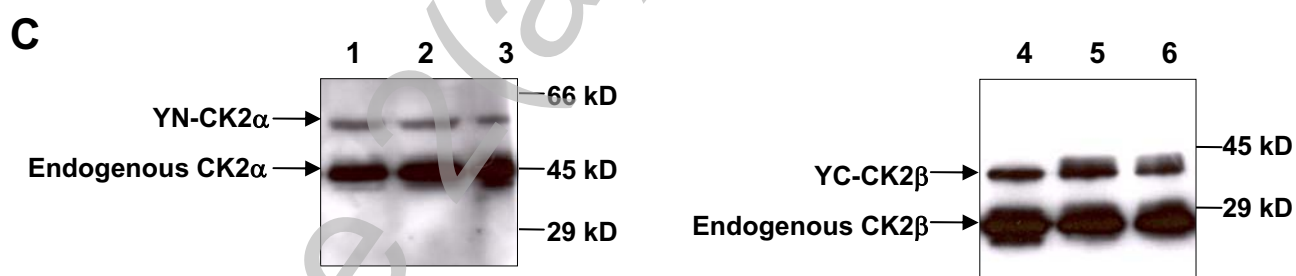


**Figure 6**

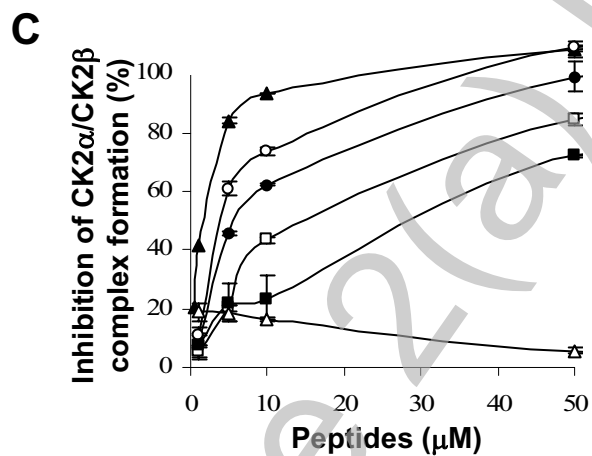
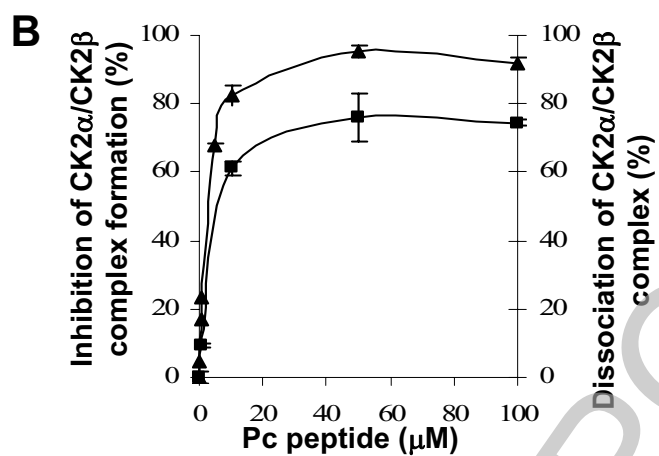
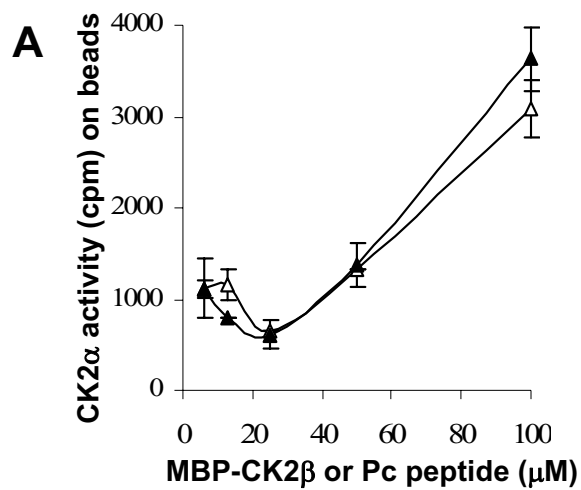
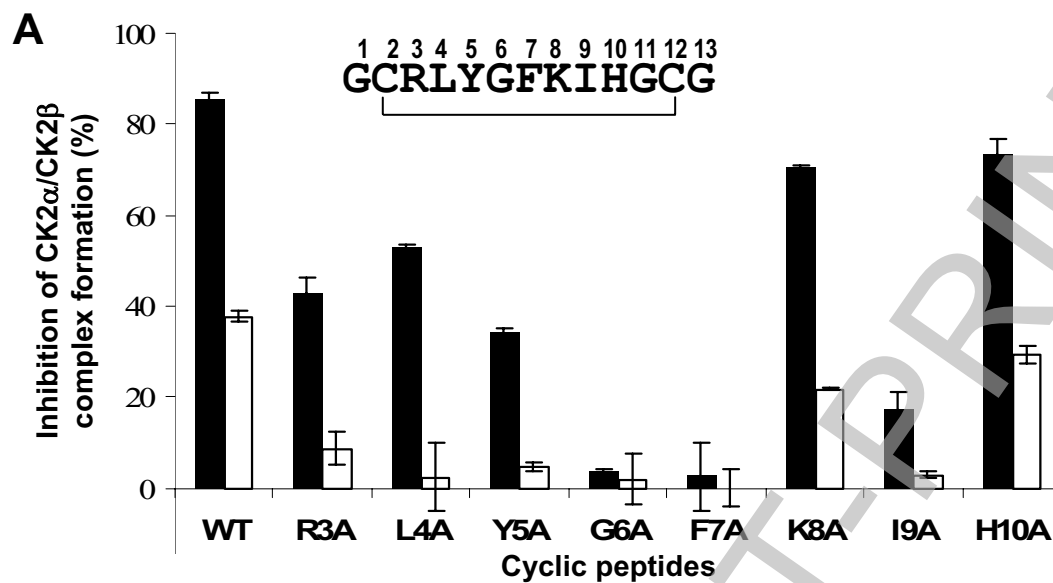
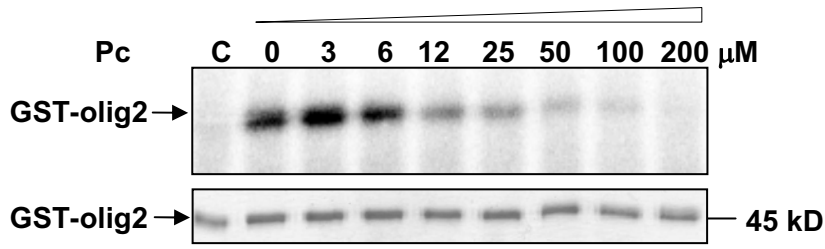


Figure 7

**B**

Cyclic peptides	IC <sub>50</sub> ( $\mu$ M)
Pc (GCRLYGFKIHGCG)	3.0
Pc-R3A (GCALYGFKIHGCG)	16.5
Pc-L4A (GCRAYGFKIHGCG)	22.0
Pc-Y5A (GCRLAGFKIHGCG)	54.0
Pc-G6A (GCRLYAFKIHGCG)	> 100.0
Pc-F7A (GCRLYGAKIHGCG)	>> 100.0
Pc-K8A (GCRLYGFAIHGCG)	6.5
Pc-I9A (GCRLYGFKAHGCG)	85.0
Pc-H10A (GCRLYGFKIAGCG)	15.0

Figure 8



**Figure 9**

Stage 2(a) POST-PRINT

THIS IS NOT THE FINAL VERSION - see doi:10.1042/BJ20070825